

Selective Synthesis of Fused Cyclooctatetraenes by [4+4] Coupling Between Two Different Diene Units

Yoshihiko Yamamoto,* Tatsuya Ohno, and Kenji Itoh^[a]

Abstract: In the presence of CuCl and 1,3-dimethyl-3,4,5,6-tetrahydro-2(1*H*)-pyrimidinone, the [4+4] coupling between zirconacyclopentadienes and 1,3-diiodobutadienes fused through an oxygen or nitrogen five-membered ring proceeded at ambient temperature to afford fully substituted polycyclic cyclo-

octatetraenes in good yields. The fused ring moiety of the diiodides plays a critical role. The corresponding acyclic

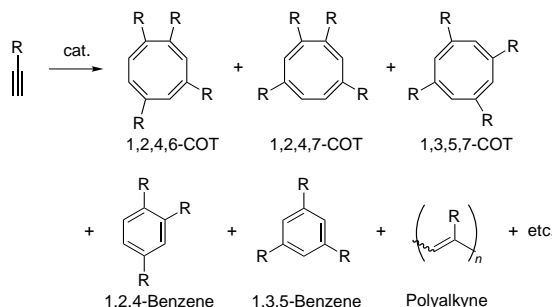
Keywords: alkynes • C–C coupling • cyclooligomerization • fused-ring systems • medium-ring compounds

diiodide and a cyclohexane-fused analogue gave no coupling product, and a cyclopentane derivative showed only moderate reactivity. Correlation of the structures of the diiodides and their reactivity was established by an X-ray and density functional study.

Introduction

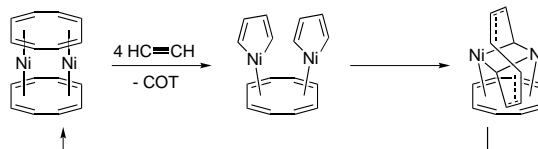
The Ni-catalyzed cyclotetramerization of alkynes is a straightforward method for providing cyclooctatetraene (COT) and its derivatives,^[1, 2] which have been attractive synthetic targets as the smallest stable member of the nonaromatic annulenes.^[3] Whereas catalytic cyclotetramerization assembles a COT ring from simple alkyne precursors in a single operation, the catalytic synthesis of substituted COTs is of limited value for the following reasons. The starting alkyne precursors are generally limited to the parent acetylene or monosubstituted alkynes, and the latter give the 1,2,4,6-, 1,2,4,7-, and 1,3,5,7-substituted isomers in a manner that depends on the alkyne employed rather than on the nature of the catalyst (Scheme 1).^[4] The cocyclotetramerization of different alkynes could result in mixtures of all the possible COTs, without chemoselectivity.^[5] The competitive cyclotrimerization or polymerization of alkyne substrates are also serious drawbacks for catalytic COT synthesis (Scheme 1).

Some 40 years after Reppe's first discovery of the Ni-catalyzed COT synthesis,^[1] Wilke proposed a fascinating mechanism for the catalytic production of COT. Two pairs of acetylene molecules undergo oxidative cyclization on two nickel centers, which are held in close proximity to each other



Scheme 1. Possible products produced by catalytic oligomerizations of monoalkynes.

by a bridging COT ligand, and the two resulting nickel-acyclopentadienes are subsequently coupled together to form a new COT ring (Scheme 2).^[6]

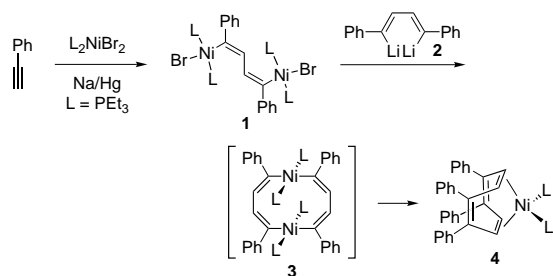


Scheme 2. Wilke's metallacyclopentadiene coupling mechanism for Ni-catalyzed cyclotetramerization of acetylene.

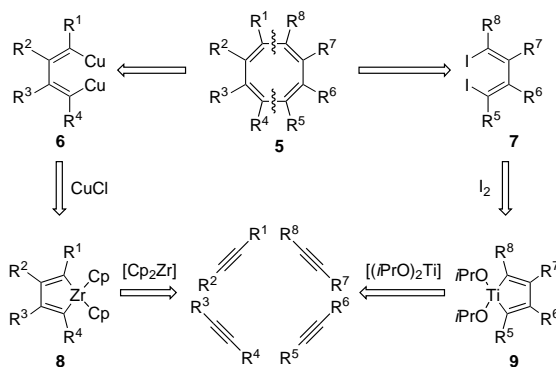
On the other hand, Carpenter and co-workers have reported an alternative COT formation via a dinickelacycle intermediate (Scheme 3).^[7] The reduction of $[(Et_3P)_2NiBr_2]$ in the presence of phenylacetylene produced a 1,4-dinickelacyclopentadiene **1**, which subsequently reacted with (*E,E*)-1,4-dithio-1,4-diphenyl-1,3-butadiene (**2**) to give η^2 -COT complex **4**. This

[a] Dr. Y. Yamamoto, T. Ohno, Prof. Dr. K. Itoh
Department of Molecular Design and Engineering,
and Department of Applied Chemistry
Graduate School of Engineering
Nagoya University, Chikusa, Nagoya 464-8603 (Japan)
Fax: (+81) 52-789-3205
E-mail: yamamoto@apchem.nagoya-u.ac.jp

Supporting information for this article is available on the WWW under <http://www.chemurj.org/> or from the author.

Scheme 3. Carpenter's synthesis of tetraphenyl-COT complex **4**.

result showed that the diene units bridging between the two nickel centers in the dinickelacycle **3** undergo reductive elimination to produce the COT ligand. Whereas these two pathways are limited to COT formation from a single alkyne component, they enabled us to postulate a new strategy to produce more complex COT rings from several alkyne components. Highly substituted COTs **5** might be chemo- and regioselectively synthesized, provided that the selective coupling between two independently prepared different metallacyclopentadienes were possible. To accomplish this, the cross-coupling of 1,4-dicupra-1,3-butadienes **6** with 1,4-diiodo-1,3-butadienes **7**—rather than the direct coupling of the parent metallacyclopentadiene counterparts **8** and **9**—was investigated (Scheme 4). The vinylcopper reagents **6** can be

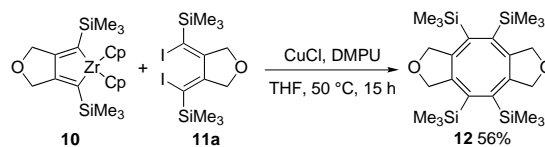


Scheme 4. Retrosynthetic scheme for construction of fully substituted COTs from four different alkynes.

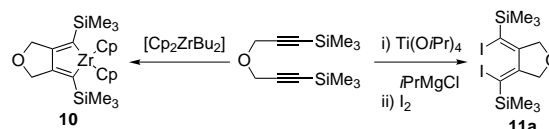
prepared by transmetalation of the corresponding zirconacyclopentadienes **8**, as reported by Takahashi and co-workers.^[8] The bifunctional electrophile diiodides **7** can readily be obtained from the corresponding titanacyclopentadienes **9** and iodine by the Tamao–Sato procedure.^[9] In this report, we wish to describe the full details of our study on the development of such a formal [4+4] metallacyclopentadiene coupling protocol to synthesize bicyclic COTs.^[10]

Results and Discussion

At the outset of this study, we examined the coupling of a stable zirconacyclopentadiene **10**^[11] with a cyclic diiodide **11a** to afford a symmetrical tricyclic COT **12** (Scheme 5). Interestingly, both the C₄-units were prepared from the common

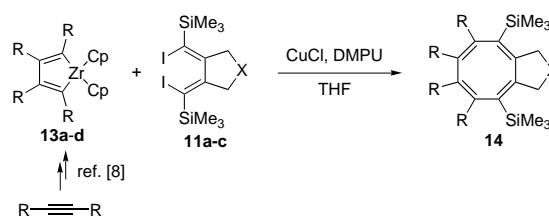
Scheme 5. Coupling of zirconacycle **10** and diiodide **11a**.

precursor 4-oxa-1,7-bis(trimethylsilyl)-1,6-heptadiyne (Scheme 6). In the presence of 3 equivalents of 1,3-dimethyl-3,4,5,6-tetrahydro-2(1*H*)-pyrimidinone (DMPU), equimolar amounts of **10** and **11a** were treated with 2.1 equiv CuCl in THF at 50 °C for 15 h. The chromatographic separation of the crude

Scheme 6. Preparation of zirconacycle **10** and diiodide **11a**.

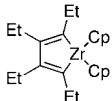
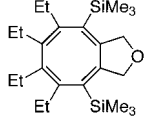
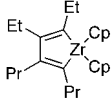
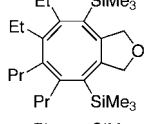
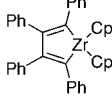
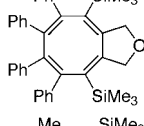
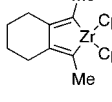
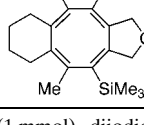
reaction mixture gave the desired product **12** in 56% yield. The structure of the COT **12** was confirmed by the following spectral data. In its ¹H NMR spectrum, only one singlet corresponding to the four trimethylsilyl groups was observed, at $\delta = 0.27$ ppm, indicative of **12** possessing a highly symmetrical structure. This was also supported by its ¹³C NMR spectrum, in which only two sp² signals were observed, at $\delta = 116.3$ and 143.3 ppm, together with a singlet for the trimethylsilyl groups and an absorption of the methylene carbon α to the ether oxygen at $\delta = -0.6$ and 70.1 ppm, respectively. The elemental analysis and the mass measurement supported this assignment (see Experimental Section).

In situ coupling of unstable zirconacyclopentadienes: The coupling of the stable, isolated zirconacyclopentadiene **10** and the diiodide **11a** having been established, unstable zirconacyclopentadienes **13a–d** were subjected to coupling with **11a** without isolation (Scheme 7). An excess of zirconacycle

Scheme 7. Coupling of zirconacycles **13a–d** with diiodides **11a–c**.

(2 equiv relative to the diiodide) was used for the in situ coupling procedure, to ensure complete consumption of the diiodide. The products and the isolated yields, together with the starting zirconacyclopentadienes, are summarized in Table 1. According to the established method,^[8] the zirconacycle **13a** (2 equiv), prepared from zirconocene dichloride and 3-hexyne, was treated with the diiodide **11a** (rt, 1 h) in the presence of CuCl (2.1 equiv) and DMPU (3 equiv) to afford the desired bicyclic COT **14aa** in 88% isolated yield.

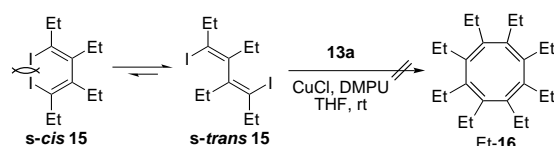
Table 1. Coupling of zirconacyclopentadienes **13a–d** with diiodide **11a**.^[a]

Zirconacyclopentadiene 13	COTs 14	Yields [%] ^[b]
 13a	 14aa	88
 13b	 14ba	79
 13c	 14ca	56
 13d	 14da	52

[a] Zirconacyclopentadiene **13** (1 mmol), diiodide **11a** (0.5 mmol), CuCl (2.1 mmol), DMPU (3 mmol), THF (5 mL), rt (50 °C for **13c**), 1 h.
 [b] Isolated yields based on **11**.

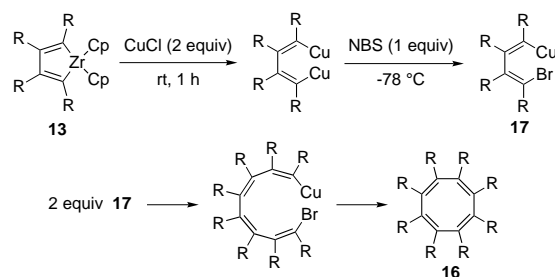
Similarly, an unsymmetrical zirconacyclopentadiene **13b**, prepared by the sequential treatment of [Cp₂Zr] with 3-hexyne and 4-octyne,^[12] reacted with **11a** without difficulty to afford an unsymmetrical COT **14ba** in 79 % yield. In contrast to these tetraalkyl-substituted zirconacycles, a tetraphenyl analogue **13c** proved less reactive at ambient temperature. Heating of the solution of **13c** with **11a** at 50 °C for 1 h, however, furnished the corresponding COT **14ca** in 56 % yield. Moreover, a tricyclic COT **14da** was successfully constructed starting from 2,8-decadiyne in 52 % yield.

The cyclic structure of the diiodide **11a** plays a critical role in this [4+4] coupling. An acyclic diiodide **15**^[13] gave no coupling product under the same reaction conditions (Scheme 8). This is possibly attributable to the conformational flexibility of its butadiene moiety. The diiodobutadiene

Scheme 8. Behavior of acyclic diiodide **15**.

moiety fixed in the *s-cis* form in **11a** seems favorable for the desired coupling, whereas acyclic **15** exists mainly in the *s-trans* conformation in order to avoid the steric repulsion between the two iodine atoms (see below).

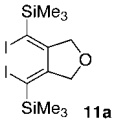
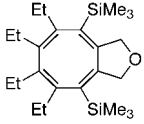
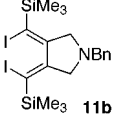
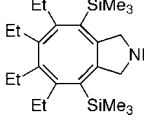
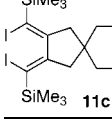
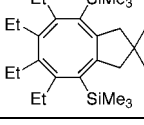
Takahashi and co-workers also reported that dihalobutadienes failed to undergo coupling with zirconacyclopentadienes **13**.^[14] Interestingly, they found that the zirconacyclopentadienes **13** cyclodimerized to give COTs **16** in 29–54 % yields upon sequential treatment with 2 equiv CuCl at rt and 1 equiv NBS at –78 °C (Scheme 9).^[14] It is noteworthy that the bromobutadienylcopper intermediates **17** successfully

Scheme 9. Takahashi's synthesis of fully substituted COTs **16**.

gave rise to the desired COTs **16**, since they have a flexible butadiene moiety very similar to that in the diiodide **15**. These facts prompted us to examine the influence of the diiodide structure on the COT formation.

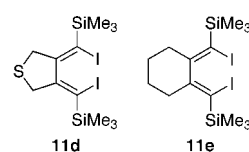
To examine the generality of this COT formation with respect to the diiodide, various hetero- and carbocyclic compounds **11b–e** were prepared from the corresponding diynes and subjected to treatment with the zirconacycle **13a** (Scheme 7, Table 2). A pyrrolidine derivative **11b**, which is an

Table 2. Coupling of zirconacyclopentadienes **13a** with diiodides **11a–c**.^[a]

Diiodide 11	COTs 14	Conditions/Yields [%] ^[b]
 11a	 14aa	rt, 1 h/88
 11b	 14ab	rt, 1 h/84
 11c	 14ac	rt, 20 h/46 50 °C, 20 h/65

[a] Zirconacyclopentadiene **13a** (1 mmol), diiodide **11** (0.5 mmol), CuCl (2.1 mmol), DMPU (3 mmol), THF (5 mL). [b] Isolated yields based on **11**.

aza-analogue of **11a**, gave the desired COT **14ab** in a yield similar to that of **14aa** under the same reaction conditions. On the other hand, a carbocyclic analogue **11c** reacted with **13a** more slowly than the heterocyclic analogues **11a** or **11b** at ambient temperature. In addition, the yield of the corresponding COT **14ac** was much lower even after stirring for 20 h. At an elevated temperature of 50 °C, the yield was improved to 65 %. In striking contrast, diiodides **11d** and **11e**, containing tetrahydrothiophene and cyclohexane rings, hardly reacted with **13a** at ambient temperature.



Three-dimensional structure determination of COT by X-ray crystallography: COT, the smallest nonaromatic annulene, preferentially exists in a nonplanar tub form (D_{2d}), which undergoes tub-inversion through a bond-localized planar form (D_{4h}) or bond-shifting through a bond-delocalized planar form (D_{8h}) as depicted in Figure 1.^[15] COTs with stable

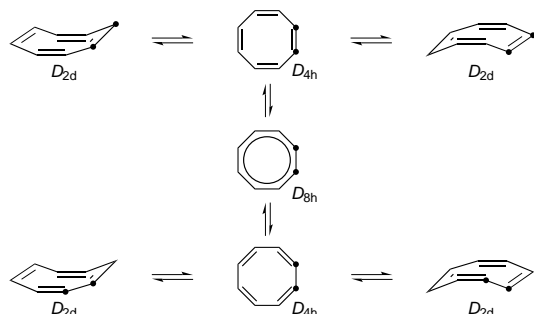
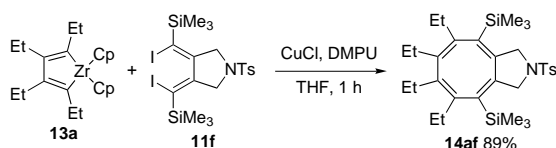


Figure 1. Dynamic conformational changes of COT.

D_{4h} conformations have also received continuous attention.^[16] To gain further information about the three-dimensional structures of the bicyclic COTs obtained from this [4+4] coupling, we carried out an X-ray diffraction study. The desired single crystal was gratifyingly obtained by the recrystallization of a tosylamide derivative **14af**, which was synthesized from the zirconacycle **13a** and the diiodide **11f** in 89% yield (Scheme 10 and Figure 2).



Scheme 10. Synthesis of COT **14af**.

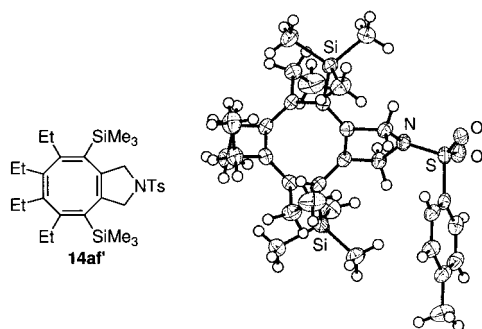


Figure 2. Solid-state structure of COT **14af**.

As shown in Figure 3, the central eight-membered ring of **14af** exists in a tub shape with four localized double bonds ($C_2=C_3$, $C_4=C_5$, $C_6=C_7$, and $C_8=C_9$). This suggests that **14af** is sufficiently conformationally stable not to isomerize to the other conformer **14af'** by bond-shifting at ambient temperature.

X-ray diffraction and density functional study on the structures of the diiodides: As described above, the cyclic diiodides

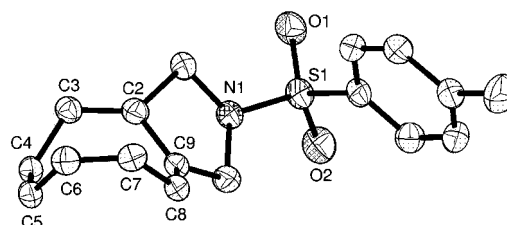


Figure 3. ORTEP diagram of COT **14af** at 50% probability level. All hydrogen atoms and substituents on the COT ring are omitted for clarity. Selected bond lengths [Å]: C_2-C_3 1.341(3), C_3-C_4 1.495(3), C_4-C_5 1.330(3), C_5-C_6 1.489(3), C_6-C_7 1.339(3), C_7-C_8 1.499(3), C_8-C_9 1.342(3), C_9-C_2 1.469(3).

11a–c with cisoid diene units reacted with the zirconacycle **13a** at room temperature to afford the COTs, although the acyclic diiodide **15** gave no coupling product under the same reaction conditions. With these results in mind, we conjectured that the *s-cis* geometry of the diiodobutadiene moiety was essential for the successful coupling. The tetrahydrothiophene or cyclohexane derivatives **11d** and **11e**, however, gave no reaction, despite undoubtedly having diiododiene moieties with *s-cis* conformations. To obtain further insight into the correlation between these structural features and the reactivity of the diiodides, we attempted X-ray crystallographic analyses of the typical diiodides **11e** and **11f**. The ORTEP diagram of **11e**, presented in Figure 4, shows a chair-like

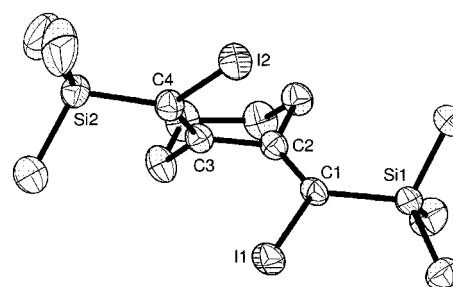


Figure 4. ORTEP diagram of COT **11e** at 50% probability level. All hydrogen atoms are omitted for clarity.

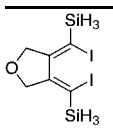
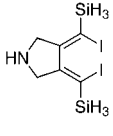
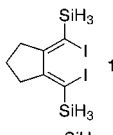
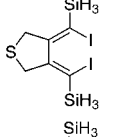
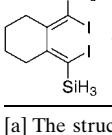
cyclohexane ring with internal angles ($108.6-111.8^\circ$) close to the expected value of 109.5° , as well as a highly skewed 1,3-diene moiety with a torsion angle of 83.3° . The two carbon–iodine single bond lengths—of 2.126(2) and 2.131(3) Å for C_1-I_1 and C_4-I_2 , respectively—are close to that expected for a Csp^2-I single bond (2.10 Å).^[17] The C_1-C_2 and C_3-C_4 bond lengths—of 1.342(4) and 1.338(4) Å, respectively—are similar to the expected $Csp^2=Csp^2$ double bond length of 1.32 Å, and the C_2-C_3 bond length of 1.485(3) Å is also consistent with that of the typical Csp^2-Csp^2 single bond (1.48 Å).^[17]

In comparison with the solid-state structure of **11e**, the most notable difference in that of **11f** (see Supporting Information) is the torsion angle of the exocyclic diene moiety. The $C_1-C_2-C_3-C_4$ dihedral angle of 67.4° is significantly smaller than that in **11e** (83.3°). This is because the smaller pyrrolidine ring makes the 1,3-diene moiety flatter than that fused by the more flexible cyclohexane ring. As a result, the $C_1-C_2-C_3$ and $C_2-C_3-C_4$ angles are forced to be larger, to reduce the steric repulsion between the iodine atoms

now placed in closer proximity to each other. On the basis of these observations, we envisioned that there might be some correlation between the torsion angle of the diene moiety in the diiodides and the yield of the corresponding COT.

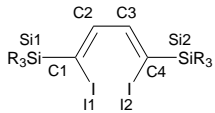
To elucidate this hypothesis, we next conducted density functional calculations at the B3LYP^[18] level for simplified model diiodides **18a–e**. At first, a cyclohexane analogue **18e** was optimized with various basis sets as summarized in Table 3, and the obtained structure was compared to that of the parent **11e** in the solid state. Initially, the structural optimization was carried out with the LANL2DZ basis set including a double- ζ basis set with the relativistic effective core potential of Hay and Wadt (LANL ECP)^[19] for I and the 6-31G(d)^[20] basis set for the rest. The optimized structure is similar to the solid-state structure of **11e** except for the longer I–Csp² bond length (2.187 Å). The I–Csp² bond was shortened to 2.155 Å by use of the LANL2DZdp basis set (LANL2DZ with one polarization and one diffuse function)^[21] for I. In this case, the C1–C2–C3–C4 dihedral angle is also closer to that of **11e**. The further calculation performed with a triple- ζ basis set combination of the SDD basis set involving the Stuttgart–Dresden–Bonn energy-consistent pseudopotential (SDB ECP)^[22] for I and the 6-311G(d)^[23] basis set gave a similar result to that obtained from the double- ζ basis sets (6-31G(d)+LANL2DZ). Finally, we carried out optimization with Dunning's correlation consistent basis set.^[24] Because it was anticipated that the addition of a f-polarization function to I would play an important role

Table 4. Calculated dihedral angles of butadiene moieties for model diiodides **18a–e** and yields of corresponding COTs **14**.^[a]

Model diiodides	Dihedral angles [°]	Yields of COTs 14 ^[b] [%]
 18a	59.87	14aa 88
 18b	59.43	14ab 84
		14af 89
 18c	68.31	14ac 46
 18d	75.66	14ad <5
 18e	83.22	14ae 0

[a] The structures of **18a–e** were optimized at the B3LYP level with the basis sets consisting of the SDB-cc-pVTZ basis set for I and the cc-pVDZ basis set for the rest. [b] Isolated yields of **14** from the reaction between the corresponding diiodides **11** and zirconacyclopentadiene **13a** at rt.

Table 3. Selected bond lengths [Å] and angles [°] in **11e**, **11f**, and **18e**.

	I1–C1 [I2–C4]	Si1–C1 [Si2–C4]	C1–C2 [C3–C4]	C2–C3	∠ C1–C2–C3 [∠ C2–C3–C4]	∠ C1–C2–C3–C4
						
11e	2.126(2)	1.888(3)	1.342(4)	1.485(3)	126.2(2)	83.3
X-ray	[2.131(3)]	[1.880(3)]	[1.338(4)]		[125.7(2)]	
18e						
6-31G(d)+LANL2DZ	2.187	1.880	1.340	1.490	120.06	84.53
6-31G(d)+LANL2DZdp	2.155	1.880	1.340	1.490	125.77	83.94
6-311G(d)+SDD	2.189	1.870	1.330	1.490	125.93	84.90
cc-pVDZ+SDB-cc-pVTZ	2.128	1.890	1.340	1.490	125.58	83.22
11f	2.112(3)	1.900(3)	1.336(4)	1.484(3)	130.6(2)	67.4
X-ray	[2.116(3)]	[1.891(3)]	[1.340(4)]		[131.1(3)]	

in the system, we decided to use a triple- ζ basis set. To this end, the recently reported SDB-cc-pVTZ^[25] basis set consisting of the [3s3p2d1f] contracted basis set and the SDB pseudopotential was employed for I. The valence double- ζ basis sets (cc-pVDZ) were assigned to the other elements. Gratifyingly, the resultant structural features—including the I–Csp² bond length (2.128 Å) and the C1–C2–C3–C4 dihedral angle (83.22°)—are very similar to those of **11e**.

After the basis sets were optimized, other model diiodides **18a–d** were investigated by DFT calculations. The calculated dihedral angles of the diene moieties in the model systems and the yields of the corresponding COTs **14aa–14af** at room temperature are compiled in Table 4. As expected, the

reactivity of the diiodides clearly varies depending on the fused ring. For the oxygen and nitrogen five-membered heterocycles **18a** and **18b**, the dihedral angles were calculated as 59.87 and 59.43°, respectively. From the parent heterocyclic diiodides, the corresponding COTs were produced in more than 80% yield. As the angle slightly increases to 68.31° in the cyclopentane analogue **18c**, the yield of the COT dramatically decreases from ca. 80% for **14aa**, **14ab**, and **14af** to 46% for **14ac**. The dihedral

angles were estimated as over 70° for the analogues bearing larger rings such as tetrahydrothiophene or cyclohexane, and the corresponding COTs were hardly obtained.

Conclusion

In conclusion, we have developed a novel strategy to assemble COTs by [4+4] coupling of zirconacyclopentadienes and 1,4-diiodo-1,3-butadienes. This approach enables us to synthesize unsymmetrical fused COTs with complete chemo- and regioselectivity, starting from several different alkynes. X-ray crystallography found that the obtained COTs exist in

a tub-shape conformation without bond-shifting isomerization. The structure of the diiodides plays a decisive role for the successful formation of COTs. The reactivity of the diiodides decreased in the following order: tetrahydrofuran-fused **11a** \cong pyrrolidine-fused **11b** > cyclopentane-fused **11c** \gg cyclohexane-fused **11e** \cong acyclic **15**. DFT calculations on the model systems showed that a flatter diiodide gave the desired COT in better yield, and the torsion angle of the diene moiety for the reactive substrates **11a–c** was estimated as $\leq 70^\circ$.

Experimental Section

General: ^1H and ^{13}C NMR were measured as CDCl_3 solutions on a Varian Mercury 300 NMR spectrometer. Chemical shifts (δ) are given in ppm relative to CDCl_3 , and coupling constants (J) in Hz. Mass spectra were recorded on a JEOL JMS-AX 505 HA mass spectrometer. Elemental analyses were performed by the Microanalytical Center of Kyoto University. Melting points were obtained on a Büchi Melting Point B-540 and are uncorrected. Flash chromatography (FC) was performed with a silica gel column (Merck silica gel 60) eluted with mixed solvents [hexane/AcOEt]. THF was distilled from CaH_2 , and degassed.

Starting materials: Zirconocene dichloride and titanium tetrakisopropoxide were purchased and used without further purification. Zirconacyclopentadienes **10**^[11] and **13a–d**,^[8] and diiodides **11a–d**^[9] and **15**^[13] were prepared by the reported procedures. Diiodides **11e** and **15** were reported in refs. 9 and 13, respectively.

Analytical data for 11a: m.p. 71–72 °C; FC: hexane/AcOEt 20:1; ^1H NMR (300 MHz, CDCl_3 , 25 °C): δ = 0.29 (s, 18H), 4.30 (br d, J = 9.3 Hz, 2H), 4.45 (br d, J = 9.3 Hz, 2H); ^{13}C NMR (75 MHz, CDCl_3 , 25 °C): δ = 0.53, 69.66, 108.46, 155.92; MS (FAB): m/z (%): 492 (11) $[M]^+$, 477 (16) $[M - \text{CH}_3]^+$, 365 (100) $[M - \text{I}]^+$; elemental analysis calcd (%) for $\text{C}_{12}\text{H}_{22}\text{I}_2\text{OSi}_2$ (492.28): C 29.28, H 4.50; found C 29.27, H 4.51.

Analytical data for 11b: m.p. 107–108 °C; FC: hexane/AcOEt 30:1; ^1H NMR (300 MHz, CDCl_3 , 25 °C): δ = 0.24 (s, 18H), 3.39 (d, J = 11.2 Hz, 2H), 3.44 (d, J = 11.4 Hz, 2H), 3.65 (d, J = 12.3 Hz, 1H), 3.72 (d, J = 12.3 Hz, 1H), 7.28–7.34 (m, 5H); ^{13}C NMR (75 MHz, CDCl_3 , 25 °C): δ = 0.76, 59.96, 60.86, 106.69, 127.28, 128.37, 128.63, 137.96, 157.47; MS (FAB): m/z (%): 582 (100) $[M + \text{H}]^+$, 454 (99) $[M - \text{I}]^+$; elemental analysis calcd (%) for $\text{C}_{10}\text{H}_{29}\text{I}_2\text{NSi}_2$ (581.42): C 39.25, H 5.03, N 2.41; found C 38.99, H 4.89, N 2.13.

Analytical data for 11c: m.p. 99–101 °C; FC: hexane/AcOEt 30:1; ^1H NMR (300 MHz, CDCl_3 , 25 °C): δ = 0.30 (s, 18H), 1.42 (s, 6H), 2.08 (d, J = 14.4 Hz, 2H), 2.56 (d, J = 14.4 Hz, 2H), 3.57 (d, J = 11.4 Hz, 2H), 3.61 (d, J = 11.4 Hz, 2H); ^{13}C NMR (75 MHz, CDCl_3 , 25 °C): δ = 1.09, 23.76, 37.69, 39.30, 68.35, 98.00, 104.82, 159.56; MS (FAB): m/z (%): 589 (52) $[M - \text{H}]^+$, 575 (100) $[M - \text{CH}_3]^+$; elemental analysis calcd (%) for $\text{C}_{18}\text{H}_{32}\text{I}_2\text{O}_2\text{Si}_2$ (590.43): C 36.62, H 5.46; found C 36.64, H 5.44.

Analytical data for 11d: m.p. 76–77 °C; FC: hexane/AcOEt 30:1; ^1H NMR (300 MHz, CDCl_3 , 25 °C): δ = 0.32 (s, 18H), 3.33 (d, J = 11.5 Hz, 2H), 3.52 (d, J = 11.5 Hz, 2H); ^{13}C NMR (75 MHz, CDCl_3 , 25 °C): δ = 1.17, 30.08, 108.29, 156.18; MS (FAB): m/z (%): 493 (10) $[M - \text{CH}_3]^+$, 381 (100) $[M - \text{I}]^+$; elemental analysis calcd for $\text{C}_{18}\text{H}_{22}\text{I}_2\text{SSi}_2$ (508.35): C 28.35, H 4.36; found C 28.15, H 4.27.

Analytical data for 11f: m.p. 182–186 °C; FC: hexane/AcOEt 20:1; ^1H NMR (300 MHz, CDCl_3 , 25 °C): δ = 0.23 (s, 18H), 2.44 (s, 3H), 3.78 (d, J = 12 Hz, 2H), 4.06 (d, J = 12 Hz, 2H), 7.35 (d, J = 8.1 Hz, 2H), 7.69 (d, J = 8.1 Hz, 2H); ^{13}C NMR (75 MHz, CDCl_3 , 25 °C): δ = 0.72, 21.63, 51.03, 110.42, 127.35, 129.86, 133.74, 143.94, 152.05; MS (FAB): m/z (%): 646 (41) $[M + \text{H}]^+$, 518 (100) $[M - \text{I}]^+$, 392 (30) $[M + \text{H} - 2\text{I}]^+$; elemental analysis calcd (%) for $\text{C}_{19}\text{H}_{29}\text{I}_2\text{NO}_2\text{SSi}_2$ (645.49): C 35.35, H 4.53, N 2.17; found C 35.07, H 4.40, N 2.08.

CuCl-mediated coupling of zirconacyclopentadiene 10 with diiodide 11a: CuCl (104 mg, 1.05 mmol) and diiodide **11a** (246 mg, 0.5 mmol) were added in that order, under Ar at 0 °C, to a solution of zirconacyclopentadiene **10** (230 mg, 0.5 mmol) and DMPU (192 mg, 1.5 mmol) in dry degassed THF (2 mL). The resultant brown mixture was stirred at 50 °C for

15 h. The reaction was quenched with HCl (1N, 3 mL), and the products were extracted with ethyl acetate (10 mL \times 3). After removal of insoluble materials by filtration, the extract was washed with sat. NaHCO_3 and brine. The organic layer was dried with MgSO_4 and concentrated. The residue was purified by silica gel flash column chromatography (hexane/AcOEt 100:1) to give COT **12** (210 mg, 56 %) as a yellow oil. ^1H NMR (300 MHz, CDCl_3 , 25 °C): δ = 0.27 (s, 36H), 4.39 (d, J = 16.5 Hz, 4H), 4.44 (d, J = 16.5 Hz, 4H); ^{13}C NMR (75 MHz, CDCl_3 , 25 °C): δ = -0.6, 70.1, 116.3, 143.3; MS (FAB): m/z (%): 477 (3) $[M + \text{H}]^+$, 364 (50) $[M - \text{CH}_3\text{CCSiMe}_3]^+$, 306 (44) $[M - \text{Me}_3\text{SiCCSiMe}_3]^+$, 184 (22) $[M - 4\text{SiMe}_3]^+$, 134 (100) $[\text{C}_8\text{H}_6\text{O}_2]^+$; elemental analysis calcd (%) for $\text{C}_{24}\text{H}_{44}\text{O}_2\text{Si}_4$ (476.95): C 60.44, H 9.30; found C 60.79, H 8.95.

Typical procedure for the synthesis of COTs from zirconacyclopentadienes 13 and diiodides 11: *n*-BuLi (1.6M hexane solution, 1.25 mL, 2 mmol) was added at -78 °C to a solution of $[\text{Cp}_2\text{ZrCl}_2]$ (292 mg, 1 mmol) in dry degassed THF (5 mL). After the mixture had been stirred at -78 °C for 1 h, an alkyne (2 mmol) or a diyne (1 mmol) was added and the stirring was continued at rt for 1 h. CuCl (208 mg, 2.1 mmol), DMPU (3.6 mL, 3 mmol), and a diiodide **11** (0.5 mmol) were added, in that order and at 0 °C, to the resultant solution. After the solution had been stirred under the conditions described in Tables 1 or 2, insoluble materials were removed by filtration with Celite. The filtrate was concentrated in vacuo and the residue was purified by silica gel flash column chromatography with a hexane/AcOEt mixed solvent as an eluent to give a COT **14** in a yield indicated in Tables 1 and 2.

Spectral data for 14aa: Oil; FC: hexane/AcOEt 200:1; ^1H NMR (300 MHz, CDCl_3 , 25 °C): δ = 0.12 (s, 18H), 0.80 (t, J = 7.5 Hz, 6H), 0.95 (t, J = 7.5 Hz, 6H), 1.52 (dq, J = 15, 7.5 Hz, 2H), 1.94 (dq, J = 15, 7.5 Hz, 2H), 2.25 (dq, J = 15, 7.5 Hz, 2H), 2.44 (dq, J = 15, 7.5 Hz, 2H), 4.11 (d, J = 10.5 Hz, 2H), 4.30 (d, J = 10.5 Hz, 2H); ^{13}C NMR (75 MHz, CDCl_3 , 25 °C): δ = 0.10, 13.95, 15.51, 23.44, 25.90, 67.93, 137.62, 142.01, 142.28, 148.46; MS (FAB): m/z (%): 401 (29) $[M - \text{H}]^+$, 374 (17) $[M - \text{C}_2\text{H}_4]^+$, 328 (71) $[M - \text{H} - \text{SiMe}_3]^+$, 300 (100) $[M - \text{C}_2\text{H}_5 - \text{SiMe}_3]^+$, 270 (15) $[M - \text{H} - 2\text{C}_2\text{H}_5 - \text{SiMe}_3]^+$; elemental analysis calcd (%) for $\text{C}_{24}\text{H}_{42}\text{OSi}_2$ (402.76): C 71.57, H 10.51; found C 71.43, H 10.65.

Spectral data for 14ba: Oil; FC: hexane/AcOEt 200:1; ^1H NMR (300 MHz, CDCl_3 , 25 °C): δ = 0.11 (s, 18H), 0.80 (t, J = 7.2 Hz, 3H), 0.84 (t, J = 7.2 Hz, 3H), 0.90 (t, J = 7.2 Hz, 3H), 0.96 (t, J = 7.2 Hz, 3H), 1.00–1.25 (m, 2H), 1.37–1.61 (m, 4H), 1.88–2.03 (m, 2H), 2.10–2.47 (m, 4H), 4.13 (d, J = 10.5 Hz, 2H), 4.32 (dd, J = 10.5, 4.8 Hz, 2H); ^{13}C NMR (75 MHz, CDCl_3 , 25 °C): δ = 0.09, 0.11, 13.93, 14.32, 15.00, 15.52, 22.24, 23.55, 23.84, 25.85, 33.12, 35.00, 68.04, 137.04, 138.06, 140.35, 141.86, 142.49, 142.76, 148.29, 148.66; MS (FAB): m/z (%): 430 (88) $[M]^+$, 357 (75) $[M - \text{SiMe}_3]^+$, 327 (100) $[M - \text{H} - \text{C}_2\text{H}_5 - \text{SiMe}_3]^+$, 299 (63) $[M - \text{H} - 2\text{C}_2\text{H}_5 - \text{SiMe}_3]^+$; elemental analysis calcd (%) for $\text{C}_{26}\text{H}_{46}\text{OSi}_2$ (430.81): C 72.49, H 10.76; found C 72.35, H 10.91.

Spectral data for 14ca: Oil; FC: hexane/AcOEt 50:1; ^1H NMR (300 MHz, CDCl_3 , 25 °C): δ = 0.35 (s, 18H), 4.54 (d, J = 10.5 Hz, 2H), 4.61 (d, J = 10.5 Hz, 2H), 7.06–7.23 (m, 20H); ^{13}C NMR (75 MHz, CDCl_3 , 25 °C): δ = -0.76, 69.06, 126.11, 127.18, 127.24, 127.78, 130.96, 130.83, 140.19, 140.33, 140.47, 144.68, 146.88, 149.10; MS (FAB): m/z (%): 594 (100) $[M]^+$, 521 (50) $[M - \text{SiMe}_3]^+$, 505 (33) $[M - \text{H} - \text{CH}_3 - \text{SiMe}_3]^+$; elemental analysis calcd (%) for $\text{C}_{40}\text{H}_{42}\text{OSi}_2$ (594.93): C 80.75, H 7.12; found C 80.66, H 7.21.

Spectral data for 14da: Oil; FC: hexane/AcOEt 300:1; ^1H NMR (300 MHz, CDCl_3 , 25 °C): δ = 0.12 (s, 18H), 1.23–1.80 (m, 8H), 1.59 (s, 6H), 4.18 (d, J = 10 Hz, 2H), 4.22 (dd, J = 10 Hz, 2H); ^{13}C NMR (75 MHz, CDCl_3 , 25 °C): δ = 0.07, 19.09, 28.41, 31.69, 68.68, 130.70, 136.77, 144.88, 145.82; MS (FAB): m/z (%): 372 (100) $[M]^+$, 299 (58) $[M - \text{SiMe}_3]^+$, 283 (53) $[M - \text{H} - \text{CH}_3 - \text{SiMe}_3]^+$; elemental analysis calcd (%) for $\text{C}_{22}\text{H}_{36}\text{OSi}_2$ (372.69): C 70.90, H 9.74; found C 70.60, H 10.05.

Spectral data for 14ab: Oil; FC: hexane/AcOEt 300:1; ^1H NMR (300 MHz, CDCl_3 , 25 °C): δ = 0.08 (s, 18H), 0.82 (t, J = 7.5 Hz, 6H), 0.95 (t, J = 7.5 Hz, 6H), 1.50 (dq, J = 13.5, 7.5 Hz, 2H), 1.93 (dq, J = 13.5, 7.5 Hz, 2H), 2.23 (dq, J = 13.5, 7.5 Hz, 2H), 2.42 (dq, J = 13.5, 7.5 Hz, 2H), 3.29 (s, 2H), 3.73 (d, J = 13.5 Hz, 2H), 3.85 (d, J = 13.5 Hz, 2H), 7.10–7.40 (m, 5H); ^{13}C NMR (75 MHz, CDCl_3 , 25 °C): δ = 0.27, 14.14, 15.54, 23.37, 26.16, 55.95, 61.30, 126.17, 126.89, 128.17, 128.37, 128.49, 137.36, 141.99; MS (FAB): m/z (%): 492 (100) $[M + \text{H}]^+$, 398 (16) $[M - \text{H} - \text{CH}_3\text{Ph}]^+$; elemental analysis calcd

(%) for $C_{31}H_{49}NSi_2$ (491.90): C 75.69, H 10.04, N 2.85; found C 75.76, H 10.00, N 2.82.

Spectral data for 14ac: Oil; FC: hexane/AcOEt 300:1; 1H NMR (300 MHz, $CDCl_3$, 25 °C): δ = 0.12 (s, 18H), 0.77 (t, J = 7.5 Hz, 6H), 0.93 (t, J = 7.5 Hz, 6H), 1.43 (s, 6H), 1.44 (dq, J = 15, 7.5 Hz, 2H), 1.92 (dq, J = 15, 7.5 Hz, 2H), 1.96 (d, J = 14.7 Hz, 2H), 2.22 (dq, J = 15, 7.5 Hz, 2H), 2.36 (d, J = 14.7 Hz, 2H), 2.40 (dq, J = 15, 7.5 Hz, 2H), 3.58 (d, J = 11.1 Hz, 2H), 3.66 (d, J = 11.1 Hz, 2H); ^{13}C NMR (75 MHz, $CDCl_3$, 25 °C): δ = 0.46, 14.23, 15.45, 23.21, 23.90, 26.00, 37.71, 60.37, 69.53, 97.65, 137.12, 140.23, 141.94, 151.14; MS (FAB): m/z (%): 500 (45) $[M]^+$, 427 (100) $[M - SiMe_3]^+$; elemental analysis calcd (%) for $C_{30}H_{53}O_2Si_2$ (500.90): C 71.93, H 10.46; found C 71.77, H 10.66.

Spectral data for 14af: m.p. 152.8–153.6 °C; FC: hexane/AcOEt 20:1; 1H NMR (300 MHz, $CDCl_3$, 25 °C): δ = 0.06 (s, 18H), 0.51 (t, J = 7.5 Hz, 6H), 0.90 (t, J = 7.5 Hz, 6H), 1.35 (dq, J = 15, 7.5 Hz, 2H), 1.91 (dq, J = 15, 7.5 Hz, 2H), 2.16 (dq, J = 15, 7.5 Hz, 2H), 2.34 (dq, J = 15, 7.5 Hz, 2H), 2.40 (s, 3H), 3.69 (d, J = 11.5 Hz, 2H), 3.93 (d, J = 11.5 Hz, 2H), 7.29 (d, J = 8.5 Hz, 2H), 7.72 (d, J = 8.5 Hz, 2H); ^{13}C NMR (75 MHz, $CDCl_3$, 25 °C): δ = 0.07, 13.60, 15.46, 21.55, 23.34, 25.64, 50.02, 127.45, 129.55, 133.83, 137.80, 141.41, 143.33, 143.87, 144.62; MS (FAB): m/z (%): 556 (30) $[M+H]^+$, 400 (100) $[M+H - SO_2C_6H_4CH_3]^+$; elemental analysis calcd (%) for $C_{31}H_{49}NO_2Si_2$ (555.96): C 66.97, H 8.88, N 2.52; found C 66.69, H 9.14, N 2.41.

Crystallographic structural determinations of COT 14af and diiodides 11e and 11f (Table 5): Single crystals suitable for X-ray analysis were obtained by recrystallization from *t*BuOMe/hexane (14af), hexane (11e), or AcOEt (11f). A crystal was mounted on a glass fiber, and diffraction data were

collected at 293 K on a Bruker SMART APEX CCD diffractometer with graphite monochromatized MoK_{α} radiation (λ = 0.71073 Å). The absorption correction was performed by use of SADABS. The structure was solved by direct methods and refined by full-matrix, least-squares on F^2 with SHELXTL. All non-hydrogen atoms were refined with anisotropic displacement parameters. All hydrogen atoms were placed in calculated positions. CCDC-186 946 (14af), -186 947 (11e), and -186 948 (11f) contain the supplementary crystallographic data for this paper. These data can be obtained free of charge via www.ccdc.cam.ac.uk/conts/retrieving.html (or from the Cambridge Crystallographic Data Centre, 12, Union Road, Cambridge CB2 1EZ, UK; fax: (+44) 1223-336033; or deposit@ccdc.cam.ac.uk).

Computational methods: All calculations were performed with the Gaussian 98 package.^[26] The density functional calculations were carried out at the B3LYP level with a various combinations of basis sets. The standard basis sets such as 6-31G(d),^[20] 6-311G(d),^[23] LANL2DZ,^[19] SDD,^[22] and cc-pVDZ^[24] were used as stored in the Gaussian program. Other basis sets, LANL2DZdp^[21] and SDB-cc-pVTZ,^[25] were available from the extensible computational chemistry environment basis set database.^[27]

Acknowledgements

We gratefully acknowledge financial support in the form of a Grant-in-Aid from the Japanese Ministry of Education, Science, Sports, and Culture.

Table 5. Crystal data and structure refinement for COT 14af, diiodide 11e and diiodide 11f.

empirical formula	$C_{31}H_{49}NO_2Si_2$	$C_{14}H_{26}I_2Si_2$	$C_{19}H_{29}I_2NO_2Si_2$
F_w	555.95	504.33	645.47
T [K]	173(2)	173(2)	173(2)
λ [Å]	0.71073	0.71073	0.71073
crystal system	monoclinic	monoclinic	triclinic
space group	$P2(1)/c$	$P2(1)/n$	$P\bar{1}$
unit cell dimensions			
a	18.578(3)	12.3123(7)	11.0668(5)
b [Å]	10.0812(18)	11.5502(6)	11.6271(5)
c [Å]	18.089(3)	15.2480(8)	11.7454(5)
α [°]	90	90	64.2560(10)
β [°]	106.547(4)	112.2700(10)	76.2930(10)
γ [°]	90	90	68.8020(10)
V [Å ³]	3247.6(10)	2006.67(19)	1263.46(10)
Z	4	4	2
ρ_{calcd} [Mg m ⁻³]	1.137	1.669	1.697
μ [mm ⁻¹]	0.200	4.051	2.680
$F(000)$	1208	1220	632
crystal size [mm ³]	$0.5 \times 0.5 \times 0.5$	$0.1 \times 0.2 \times 0.8$	$0.8 \times 0.5 \times 0.2$
θ range [°]	2.29 to 23.31	1.82 to 29.17	1.93 to 29.15
index ranges	$-16 \leq h \leq 20$ $-11 \leq k \leq 11$ $-20 \leq l \leq 19$	$-16 \leq h \leq 12$ $-14 \leq k \leq 15$ $-20 \leq l \leq 20$	$-15 \leq h \leq 11$ $-15 \leq k \leq 15$ $-15 \leq l \leq 16$
refls collected	15 705	15 470	10 052
independent refls	4684 [$R(\text{int}) = 0.0215$]	5386 [$R(\text{int}) = 0.0413$]	6688 [$R(\text{int}) = 0.0263$]
completeness to θ [°] [%]	23.31 99.5	29.17 99.4	29.15 98.3
absorption correction	empirical (SADABS)	empirical (SADABS)	empirical (SADABS)
refinement method	full-matrix, least-squares on F^2	full-matrix, least-squares on F^2	full-matrix, least-squares on F^2
data/restraints/parameters	4684/0/345	5386/0/169	6688/0/251
Gof on F^2	0.517	0.777	0.842
final R indices [$I > 2\sigma(I)$]			
R_1	0.0357	0.0318	0.0399
wR_2	0.1067	0.0853	0.1093
R indices (all data)			
R_1	0.0416	0.0359	0.0435
wR_2	0.1211	0.0885	0.1124
largest diff. peak and hole [e Å ⁻³]	0.312/−0.195	1.033/−0.790	1.960/−2.207

- [1] W. Reppe, O. Schlichting, K. Klager, T. Toepel, *Justus Liebigs Ann. Chem.* **1948**, 560, 1–92.
- [2] For a review, see: P. W. Jolly, in *Comprehensive Organometallic Chemistry*, Vol. 8 (Eds.: G. Wilkinson, F. G. A. Stone, E. W. Abel), Pergamon, London, **1982**, Chapter 56.3, p. 649–670.
- [3] For a review, see: L. A. Paquette, *Tetrahedron* **1975**, 31, 2855–2883.
- [4] a) J. R. Leto, *J. Am. Chem. Soc.* **1961**, 83, 2944–2951; b) P. Chini, N. Palladino, A. Santambrogio, *J. Chem. Soc. (C)* **1967**, 836–840; c) H. tom Dieck, M. Svoboda, J. Kopf, *Z. Naturforsch.* **1978**, 33b, 1381–1385; d) R. Diercks, L. Stamp, J. Kopf, H. tom Dieck, *Angew. Chem.* **1984**, 96, 891–895; *Angew. Chem. Int. Ed. Engl.* **1984**, 23, 893–894; e) R. Diercks, L. Stamp, H. tom Dieck, *Chem. Ber.* **1984**, 117, 1913–1919; f) R. Diercks, H. tom Dieck, *Chem. Ber.* **1985**, 118, 428–435; g) H. tom Dieck, A. M. Lauer, L. Stamp, R. Diercks, *J. Mol. Catal.* **1986**, 35, 317–328; h) W. Schulz, U. Rosenthal, D. Braun, D. Walther, *Z. Chem.* **1987**, 27, 264–265; i) D. Walther, D. Braun, W. Schulz, U. Rosenthal, *Z. Chem.* **1989**, 29, 293–294; j) D. Walther, D. Braun, W. Schulz, U. Z. Rosenthal, *Z. Anorg. Allg. Chem.* **1989**, 577, 270–282.
- [5] Cocyclotetramerizations of substituted alkynes with acetylene have been reported, see: a) A. C. Cope, H. C. Campbell, *J. Am. Chem. Soc.* **1951**, 73, 3536–3537; b) A. C. Cope, H. C. Campbell, *J. Am. Chem. Soc.* **1952**, 74, 179–183; c) A. C. Cope, D. S. Smith, *J. Am. Chem. Soc.* **1952**, 74, 5136–5139; d) A. C. Cope, D. F. Rugen, *J. Am. Chem. Soc.* **1953**, 75, 3215–3219; e) A. C. Cope, R. M. Pike, *J. Am. Chem. Soc.* **1953**, 75, 3220–3223.
- [6] G. Wilke, *Pure Appl. Chem.* **1978**, 50, 677–690.
- [7] C. J. Lawrie, K. P. Gable, B. K. Carpenter, *Organometallics* **1989**, 8, 2274–2276.
- [8] T. Takahashi, M. Kitora, R. Hara, Z. Xi, *Bull. Chem. Soc. Jpn.* **1999**, 72, 2591–2602, and references therein.
- [9] S. Yamaguchi, R.-Z. Jin, K. Tamao, F. Sato, *J. Org. Chem.* **1998**, 63, 10060–10062.
- [10] Preliminary results have been reported: Y. Yamamoto, T. Ohno, K. Itoh, *Chem. Commun.* **1999**, 1543–1544.
- [11] F. Mohamadi, M. M. Spees, *Organometallics* **1992**, 11, 1398–1400.
- [12] Z. Xi, R. Hara, T. Takahashi, *J. Org. Chem.* **1995**, 60, 4444–4448.
- [13] C. Xi, S. Huo, T. H. Afifi, R. Hara, T. Takahashi, *Tetrahedron Lett.* **1997**, 38, 4099–4102.
- [14] T. Takahashi, W.-H. Sun, K. Nakajima, *Chem. Commun.* **1999**, 1595–1596.
- [15] L. A. Paquette, *Acc. Chem. Res.* **1993**, 26, 57–62, and references therein.
- [16] a) N. Z. Huang, F. Sondheimer, *Acc. Chem. Res.* **1982**, 15, 96–102; b) A. Matsuura, K. Komatsu, *J. Am. Chem. Soc.* **2001**, 123, 1768–1769; c) K. K. Baldrige, J. S. Siegel, *J. Am. Chem. Soc.* **2001**, 123, 1755–1759, and references therein.
- [17] M. B. Smith, J. March, *March's Advanced Organic Chemistry* (5th ed.), Wiley, New York, **2001**, Part 1, Chapter 1, p. 20.
- [18] a) W. Kohn, A. D. Becke, R. G. Parr, *J. Phys. Chem.* **1996**, 100, 12974–12980; b) P. J. Stephen, F. J. Devlin, C. F. Chabalowski, M. J. Frisch, *Phys. Chem. Lett.* **1994**, 98, 11623–11627; c) A. D. Becke, *J. Chem. Phys.* **1993**, 98, 5648–5652; d) A. D. Becke, *Phys. Rev. A* **1988**, 38, 3098–3100; e) C. Lee, W. Yang, R. G. Parr, *Phys. Rev. B* **1988**, 37, 785–789.
- [19] a) P. J. Hay, W. R. Wadt, *J. Chem. Phys.* **1985**, 82, 270–283; b) W. R. Wadt, P. J. Hay, *J. Chem. Phys.* **1985**, 82, 284–298; c) P. J. Hay, W. R. Wadt, *J. Chem. Phys.* **1985**, 82, 299–310.
- [20] a) W. J. Hehre, R. Ditchfield, J. A. Pople, *J. Chem. Phys.* **1972**, 56, 2257–2261; P. C. Hariharan, J. A. Pople, *Theor. Chim. Acta* **1973**, 28, 213–222; c) M. M. Francl, W. J. Pietro, W. J. Hehre, J. S. Binkley, M. S. Gordon, D. J. DeFrees, J. A. Pople, *J. Chem. Phys.* **1982**, 77, 3654–3665.
- [21] C. E. Check, T. O. Faust, J. M. Bailey, B. J. Wright, T. M. Gilbert, L. S. Sunderlin, *J. Phys. Chem.* **2001**, 105, 8111–8116.
- [22] A. Bergner, M. Dolg, W. Küchle, H. Stoll, H. Preuss, *Mol. Phys.* **1993**, 80, 1431–1441.
- [23] R. Krishnan, J. S. Binkley, R. Seeger, J. A. Pople, *J. Chem. Phys.* **1980**, 72, 650–654.
- [24] A. K. Wilson, D. E. Woon, K. A. Peterson, T. H. Dunning Jr., *J. Chem. Phys.* **1999**, 110, 7667–7676.
- [25] J. M. L. Martin, A. Sundermann, *J. Chem. Phys.* **2001**, 114, 3408–3420.
- [26] *Gaussian 98*, Rev. A.11, M. J. Frisch, G. W. Trucks, H. B. Schlegel, G. E. Scuseria, M. A. Robb, J. R. Cheeseman, V. G. Zakrzewski, J. A. Montgomery Jr., R. E. Stratmann, J. C. Burant, S. Dapprich, J. M. Millam, A. D. Daniels, K. N. Kudin, M. C. Strain, O. Farkas, J. Tomasi, V. Barone, M. Cossi, R. Cammi, B. Mennucci, C. Pomelli, C. Adamo, S. Clifford, J. Ochterski, G. A. Petersson, P. Y. Ayala, Q. Cui, K. Morokuma, P. Salvador, J. J. Dannenberg, D. K. Malick, A. D. Rabuck, K. Raghavachari, J. B. Foresman, J. Cioslowski, J. V. Ortiz, A. G. Baboul, B. B. Stefanov, G. Liu, A. Liashenko, P. Piskorz, I. Komaromi, R. Gomperts, R. L. Martin, D. J. Fox, T. Keith, M. A. Al-Laham, C. Y. Peng, A. Nanayakkara, M. Challacombe, P. M. W. Gill, B. Johnson, W. Chen, M. W. Wong, J. L. Andres, C. Gonzalez, M. Head-Gordon, E. S. Replogle, J. A. Pople, Gaussian, Inc., Pittsburgh PA, **2001**.
- [27] Basis sets were obtained from the Extensible Computational Chemistry Environment Basis Set Database, Version 4/05/02, as developed and distributed by the Molecular Science Computing Facility, Environmental and Molecular Sciences Laboratory, which is part of the Pacific Northwest Laboratory, P.O. Box 999, Richland, Washington 99352 (USA), and funded by the US Department of Energy. The Pacific Northwest Laboratory is a multi-program laboratory operated by the Battelle Memorial Institute for the US Department of Energy under contract DE-AC06-76RLO 1830. Contact David Feller or Karen Schuchardt for further information.

Received: June 6, 2002 [F4159]